Quantifying unitary flow efficiency and entanglement for many-body localization

Gregory A. Hamilton [*] and Bryan K. Clark

*Institute for Condensed Matter Theory and IQUIST and Department of Physics, University of Illinois at Urbana-Champaign,
Urbana, Illinois 61801, USA*

We probe the bulk geometry of the Wegner Wilson Flow (WWF) in the context of many-body localization by addressing efficiency and bulk entanglement growth measures through approximating upper bounds on the boundary entanglement entropy. We connect these upper bounds to the Fubini-Study metric and clarify how a central quantity, the information fluctuation complexity, distinguishes bulk unitary rotation from entanglement production. We also give a short new proof of the small incremental entangling theorem in the absence of ancillas, achieving a dimensionindependent, universal factor of $c = 2$.

I. INTRODUCTION

Many-body localization (MBL) is centrally a failure to thermalize [1–3]. At a phenomenological level, MBL is described by an emergent, macroscopic set of quasilocal integrals of motion, known colloquially as ℓ bits [2,4,5]. The emergence of these ℓ bits give rise to a myriad of effects, including vanishing conductivity, logarithmic entanglement growth, and area-law eigenstates [1,6,7]. Constructing ℓ bits from local operators via a diagonalizing unitary U establishes the stability of the MBL phase and yields insight on the dynamics of local observables [3,8–16].

Considerable effort has been devoted in recent years toward finding appropriate ℓ-bit construction methodologies, including strong-disorder renormalization flows, perturbative constructions, and infinite-time averaged local observables [2,6,8,17]. One recent approach, the Wegner Wilson flow (WWF), leverages a continuous renormalization flow that generally produces more quasilocal ℓ bits [17,18]. The WWF renormalization technique has been successfully used to describe the flow of coupling constants, local observables, and correlation lengths across the MBL phase transition [18,19]. As the WWF can be applied to ergodic or nonergodic Hamiltonians, the breakdown of ergodicity upon entering the area-law, MBL phase implies an efficient tensor network construction of both eigenstates and ℓ bits [20,21]. We give a full description of the WWF in Sec. IV, but fundamentally the renormalization flow is quite simple: given a Hamiltonian H written in a basis $\{|\phi_0\rangle\}$, the equation of motion reads

$$\frac{dH}{d\beta} = [\eta(\beta), H(\beta)], \quad \eta(\beta) = [H_d(\beta), H(\beta)], \quad (1)$$

where H_d is the diagonal part of the Hamiltonian in the basis $\{|\phi_0\rangle\}$.

Following this intuition, recent works implemented tensor network versions of the WWF [22,23]. Apart from the computational advantage, tensor networks offer a framework for spacetime geometry to emerge from quantum information [24]. Using this tensor network picture, we envision a generic Hamiltonian H as describing *boundary* degrees of freedom, while the unitary U that diagonalizes H represents the *bulk*. If H is expressed in some product state orthonormal basis, then the bulk unitary U effectively rotates the basis states into eigenstates of H. Thus, $U^\dagger$ *disentangles* eigenstates into product states; the geometry of the bulk tensor network should then inform the eigenstate entanglement structure. Apart from this tensor network description, the WWF has strong ties to quantum geometry and geodesicity in the projective Hilbert space [25,26], as we later explore.

The idea that tensor networks describe a quantum-informational bulk geometry is particularly relevant with respect to the Ryu-Takayanagi (RT) conjecture, frequently considered in the context of holographic tensor networks and continuous multiscale renormalization ansatzes (cMERAs) [27–32]. For such systems the bulk-boundary (AdS/CFT) correspondence we broadly invoked above is rigorous: the boundary entanglement corresponds to the area of the RT surface in the bulk [29]. The AdS/CFT correspondence and RT conjecture are foundational to the study of holographic quantum error correction [27].

However, this connection between the *bulk* geometry of U and the entanglement of the *boundary* eigenstates is much less clear in a generic tensor network construction. A notion of a gravitational theory in the bulk is not welldefined for area law states, though several recent works investigated RT-esque surfaces in bulk tensor networks that bound the boundary entanglement [33]. Minimal surfaces in the bulk have also been wellexplored in the context of random unitary circuits, wherein Haar averaging and the Weingarten calculus affords a mapping to statistical models of entanglement growth [34]. While we nonrigorously use the terms "bulk" and "boundary," it is evident that a quantum geometrical picture for a diagonalizing unitary U should shed insight on entanglement growth for the eigenstates of H.

In this work, we formalize this intuition by examining bulk measures derived from the WWF or any other continuously diagonalizing unitary U, with a focus on understanding

*gah4@illinois.edu

entanglement growth via the WWF across the many-body localized phase transition. In particular, our objective is to identify bounds on the entanglement entropy of boundary eigenstates via functionals of the bulk unitary U. We begin by examining not a bulk geometry, but rather a speed limit for the entanglement entropy. We use the small incremental entangling (SIE) theorem as a starting point to probe the entanglement structure and efficiency of unitary flows. Along the way, we give a simplified proof of the ancilla-free version of the SIE, and achieve a tighter bound than the state of the art. Inspired by the RT conjecture, which connects the boundary entanglement with distances in the holographic bulk, we demonstrate how the SIE theorem identifies computable bulk metrics intimately tied to notions of efficiency and quantum complexity.

We then apply the SIE theorem and our bulk metrics to the WWF in the context of an MBL system. We show that the WWF is monotonically more efficient upon entering the MBL phase, and that the boundary entanglement entropy monotonically decreases with efficiency. What is more, we show that some bulk metrics, while easily computable, fail to fully diagnose the flow entanglement dynamics. We identify a key quantity, the information fluctuation complexity, as a source of this failure.

II. ENTANGLEMENT SPEED LIMITS

As noted above, the RT conjecture concerns bulk geometries specified by a renormalization flow; it states that geodesics in the bulk theory directly relate to the boundary entanglement [35]. Oftentimes, a unitary flow (e.g., Hamiltonian evolution) is parametrized as a function of RG time. A natural route towards bounding entanglement entropy in the spirit of RT is therefore to bound the entropic speed limit. This prescription is central to proving the stability of the area law for one-dimensional systems [36], as well as the logarithmic lightcone and entanglement spread in MBL systems [6].

The small incremental entangling theorem (SIE), first posited by Kitaev [37], gives an upper bound on the entanglement entropy rate of a pure state under unitary evolution:

$$|\dot{E}(\rho(t))| \leqslant c||H(t)||_\infty \ln d_A, \quad c \in \mathcal{O}(1). \quad (2)$$

Here $E(\rho(t)) := S(\rho_A(t))$ denotes the entanglement entropy, $|| \cdot ||_\infty$ the operator norm, and d_A the Hilbert space dimension of subsystem $\mathcal{H}_A$. The operator $H(t)$ is the generator of unitary evolution. The most general form of the SIE theorem involves ancillary qudits [36,37], which we do not consider here. Note that if we define $H := H_A + H_{A^c} + H_\partial$, then Eq. (2) depends only on the interaction term H_∂, where we assume H_A, H_{A^c} are Hamiltonian terms local to subsystem A and its complement. However, as we detail below, in the context of the WWF $H_\partial(t)$ becomes increasingly difficult to extract from $H(t)$.

Proving the general SIE theorem has a long history, starting with Bravyi's work [37] and culminating with a proven bound $c = 18$ [36]. Since then, several works established tighter bounds on c for the ancilla-assisted case-extensively detailed in Ref. [38] numerical work suggesting an optimal value $c = 2$ both with and without ancillas. In the no-ancilla case, Bravyi's original proof yielded a $c(d)$ bound with $c(d) \to$

1 as $d \to \infty$ [37]. More recently, a bound was given for no-ancilla SIE with $c = 4$, independent of dimension d and valid for mixed states [39]. We offer a short proof here for the no-ancilla SIE that easily achieves a bound $c = 2$ valid for mixed states.

We now detail our proof for no-ancilla SIE. Let ρ be a normalized density matrix acting on a Hilbert space $\mathcal{H} \cong \mathcal{H}_A \otimes \mathcal{H}_{A^c}$. We take H to be time independent for the moment and assume $d_A \leqslant d_{A^c}$, where d_A denotes the Hilbert space dimension. The entanglement rate is quickly derived as

$$|\dot{E}(\rho(t))| = |\text{Tr}\rho(t)[H, \ln \rho_A(t) \otimes 1_{A^c}]|. \quad (3)$$

The Robertson-Schrodinger uncertainty relation then implies

$$|\text{Tr}\rho(t)[H, Y(t)]| \leqslant 2\sigma_H(t)\sigma_Y(t), \quad (4)$$

where $Y(t) := \ln \rho_A(t) \otimes 1_{A^c}$. Here $\sigma_X^2 = \text{Tr}\rho(t)X^2 - (\text{Tr}\rho(t)X)^2 \leqslant ||X||_\infty^2$ for Hermitian X, with $|| \cdot ||_\infty$ denoting the operator norm. The variance

$$\sigma_Y^2(t) = \text{Tr}_A\rho_A(t)\log^2 \rho_A(t) - (\text{Tr}_A\rho_A(t)\ln \rho_A(t))^2 \quad (5)$$

is also known as the information fluctuation complexity (IFC) for the probability distribution $\boldsymbol{p}$, where $\boldsymbol{p}$ is the spectrum of ρ_A [40]. We assume $\boldsymbol{p}$ has $n \leqslant d_A$ nonzero components, where d_A denotes the Hilbert space dimension of A. Then $\sigma_Y^2 \leqslant \sum_{i=1}^n p_i \log^2 p_i = M_n^{(2)}$, the second moment of the self-information $\ln p$. To bound the IFC, we follow and considerably simplify an approach first given in Ref. [41]. Using the normalization condition $\sum_i p_i = 1$, we define $p_n = 1 - \sum_{i=1}^{n-1} p_i$. Simple calculus yields

$$\frac{\partial M_n^{(2)}}{\partial p_i} = (a_i - a_n)(a_i + a_n - 2), \quad (6)$$

where $a_i := -\ln p_i$. Clearly maxima of $M_n^{(2)}$ vanish for each of the $n - 1$ instances of Eq. (6). The solutions $a_i = a_n$ for all i implies the trivial solution $\boldsymbol{p} = (1/n, \ldots, 1/n)$. In the case $n = 2$, we find $p_1 = \frac{1}{2}(1 + \sqrt{1 - 4e^{-2}})$ is maximal. In this case one can easily check $\ln 2$ is an upper bound for $M_n^{(2)}$.

Our goal now is to show the trivial solution is the only maxima for $M_n^{(2)}$ when $n \geqslant 3$. We regard the set of variables p_1, p_2, r with $p_n = 1 - p_1 - p_2 - r$, $r \in [0, 1)$. Without loss of generality, there are two cases to consider for a nontrivial solution:

$$\text{Case 1: } p_1 = p_n, \; p_2 p_n = e^{-2},$$
$$\text{Case 2: } p_1 p_n = e^{-2}, \; p_2 p_n = e^{-2}.$$

We utilize Gröbner bases to write Case 1 as the null space of the following set of equations: $\{p_n - p_1, p_2 + r + 2p_n - 1, 2p_n^2 + (r-1)p_n + e^{-2}\}$. A check of the discriminant of the last polynomial yields $(1 - r)^2 - 8e^{-2} < 0$ for any r. For Case 2 a Gröbner basis is $\{2p_1 + r + p_n - 1, 2p_n + r + p_n - 1, p_n^2 + (r-1)p_n + 2e^{-2}\}$, with the same discriminant as before. Therefore, the uniform distribution is the only maxima of $M_n^{(2)}$ for $n \geqslant 3$. For $n \geqslant 2$ we then have $\sigma_Y^2 \leqslant \log^2 n$ and a final bound

$$|\dot{E}(\rho(t))| \leqslant 2||H||_\infty \ln d_A. \quad (7)$$

While the logarithmic dependence of Eq. (7) can be saturated [37], most states have a slow entanglement spread under the
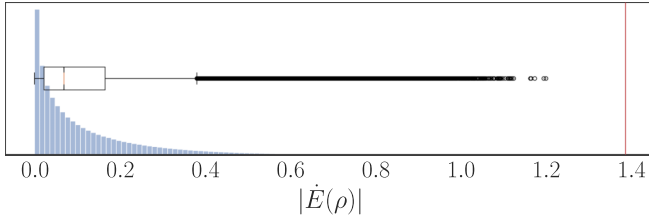
FIG. 1. Histogram and box plot of $\dot{E}(\rho)$ for a two-qubit system, over 2×10^6 realizations of pure states and Hamiltonians H, $||H||_\infty = 1$. See main text for details on the sampling. The vertical lines in the box plot reflect interquartile ranges, while the mass of points starting around 0.4 denote outliers. The red line demarcates the bound defined in the main text.

unitary evolution induced by a large ensemble of Hamiltonians [39]. In Fig. 1, we depict a histogram of two million realizations of two-qubit Hamiltonians and pure states. The Hamiltonians are generated by uniformly sampling eigenvalues from $[-1, 1]$ and then applying a Haar unitary. The pure states were generated by uniformly sampling a full rank Schmidt vector $\boldsymbol{p} = (p_1, 1 - p_1)$. The interquartile range indicates most quantum states will not saturate the SIE bound.

As noted above, the form of the SIE proven here utilizes the full Hamiltonian H, more generally, the generator for unitary evolution. The operator norm $||H||_\infty$ is in general extensive, which would imply $\dot{E}$ scales linearly with $\ln |\mathcal{H}|$. This seems paradoxical, as the entanglement entropy of A should not scale differently if $|\mathcal{H}|$ was, say, doubled while $|\mathcal{H}_A|$ remained fixed. However, it is only $H_\partial(t)$ which generates entanglement (we could always express ρ in the eigenbasis of H_A, H_{A^c}, respectively), and $||H_\partial(t)||_\infty$, assuming a local Hamiltonian, is *intensive*.

There are two reasons we focus on H instead of the entanglement-generating term H_∂. The first is theoretical: As we detail below, the generator for unitary rotations in the projective Hilbert space is H, not H_∂. As our goal is to relate the quantum geometry induced by the diagonalizing unitary U to entanglement bounds, the full generator of unitary rotations is the relevant observable. The second reason is practical. In the context of the WWF it is η from Eq. (1), not H, that dictates the unitary rotation. $\eta_\partial(\beta)$ becomes more quasilocal as a function of flow and therefore determining η_∂ via a Pauli string decomposition quickly becomes infeasible. We discuss the issue of how $||\eta_\partial||$ scales with $||\eta||$ in more detail in Sec. IV.

III. CONNECTING TO QUANTUM INFORMATION GEOMETRY

We now use the SIE theorem in Eq. (2) as a bridge to consider bulk geometry by identifying computable bulk quantities and metrics related to the flow entanglement entropy. The RT theorem indicates that minimal cuts in the bulk should be proportional to the boundary entanglement; thus, making an identification with the flow entanglement entropy helps preserve this correspondence. As we show, these bulk metrics comprise two components: A quantity related to distances in the projective Hilbert space, and the information fluctuation complexity (IFC), described above. Approximations to either

of these quantities yields a variety of bulk metrics: We find that there is a tradeoff between approximations which hew closely to the entanglement flow, and those which are easier to compute.

In this spirit we examine computable approximations to the two quantities on the RHS of Eq. (4), which we write as

$$E(\rho(t)) \leqslant 2 \int_0^t \sigma_H(t') \sigma_Y(t') dt' =: 2D_{RS} \qquad (8)$$

for initial state $\rho = |\psi\rangle \langle \psi|$.

As noted above, σ_H is less than or equal to the operator norm $||H||_\infty$, equivalent to the largest singular value $s_{\max}$ of $H^\dagger H$. Computing $||H||_\infty$ amounts to determining the extremal values of the eigenspectrum of H, which can be achieved via Lanczos or similar methods with complexity that scales as $\mathcal{O}(|\mathcal{H}|^2 \omega)$, where ω is the sparsity (average number of nonzero elements in a row) of H. In contrast, the Frobenius norm $||H||_F := \sqrt{\mathrm{Tr} H^\dagger H}$ scales as $\mathcal{O}(|\mathcal{H}|^3)$. As we describe below, $||H||_F$ is closely related to metrics on the projective Hilbert space. Leveraging the fact that $||A||_\infty \leqslant ||A||_F \leqslant \sqrt{r}||A||_\infty$ for any rank r operator A, we can approximately bound σ_H by $||H||_F/\sqrt{d}$, where $d := d_A d_{A^c} = |\mathcal{H}|$. The term $||H||_F/\sqrt{d}$ can be seen as the root of the expectation value $\langle \psi_0 | H^\dagger H | \psi_0 \rangle$, where $\{|\psi_0\rangle\}$ is an orthonormal basis for $\mathcal{H}$ chosen at the beginning of the flow.

If we now consider the *average* entanglement entropy of an initial orthonormal basis $\{|\psi_0\rangle\}$ and make the replacement $\sigma_H \to ||H||_F/\sqrt{d}$, we get

$$\langle E(\rho(t)) \rangle \lesssim \frac{2}{\sqrt{d}} \int_0^t ||H||_F \sigma_Y =: 2D_{XY}, \qquad (9)$$

where $\langle \cdot \rangle$ denotes averaging over the flowed states $\{|\psi_0(t)\rangle\}$.

Turning now to approximations for the information fluctuation complexity (IFC), we can decompose $\sigma_Y(t)$ into a running average and fluctuating component (with respect to the time parameter t), $\sigma_Y(t) = \bar{\sigma}_Y + \tilde{\sigma}_Y(t)$. Assuming $\tilde{\sigma}_Y(t) \ll \bar{\sigma}_Y$ yields

$$\langle E(\rho(t)) \rangle \lesssim \frac{2 \langle \bar{\sigma}_Y \rangle}{\sqrt{d}} \int_0^t dt' ||H(t')||_F = 2 \langle \bar{\sigma}_Y \rangle D_X, \qquad (10)$$

where we have defined

$$D_X(t) := \frac{1}{\sqrt{d}} \int_0^t dt' ||H(t')||_F. \qquad (11)$$

We interpret D_X, first suggested as a bulk metric in the context of the WWF in Ref. [22], as quantifying the average strength of rotation induced by the unitary process, integrated with respect to the flow. The term D_X is, for traceless H, the arc length of the unitary U under a standard bi-invariant Riemannian metric [42]. Different metric choices that penalize many-qubit Hamiltonian operators give rise to a geometrical notion of quantum circuit complexity [42,43].

To summarize our analysis so far, we can place bounds on the average entanglement entropy of initial orthonormal states $\{|\psi_0\rangle\}$ evolving under a Hamiltonian (or generator of unitary rotation) H using Eq. (4). The terms in Eq. (4) can be approximated by taking norms and functionals of operators through the course of the unitary flow. Cruder approximations, as we will see in Sec. IV, lead to worse bounds on the entanglement

TABLE I. Approximations to each term in Eq. 4 for the bulk metrics (D_{RS}, D_{XY}, D_X).

Bulk metric	Approx. to σ_H	Approx. to σ_Y
D_{RS}	σ_H	σ_Y
D_{XY}	$\|\|H\|\|_F/\sqrt{d}$	σ_Y
D_X	$\|\|H\|\|_F/\sqrt{d}$	$\langle \overline{\sigma}_Y \rangle$

entropy. Table I depicts the approximations made to Eq. (4) for each bulk measure.

In addition to contributing to the entanglement bounds in Eq. (4), we can relate σ_H to the *efficiency* of the unitary flow. Note that for pure state $\rho = |\psi\rangle\langle\psi|$ the term $\sigma_H^2 \equiv g_{tt}$ is simply the diagonal part of the Fubini-Study metric, $g_{\mu\nu} = \Re(Q_{\mu\nu})$ under unitary evolution $U(t)$ where $Q_{\mu\nu}$ is the quantum geometric tensor defined as

$$Q_{\mu\nu} \equiv \langle \partial_\mu \psi | (1 - |\psi\rangle\langle\psi|) |\partial_\nu \psi \rangle. \quad (12)$$

The imaginary part of $Q_{\mu\nu}$ is then proportional to the Berry curvature [44]. Note that in general μ, ν denote parameters for the state $\psi(t)$; in our case the only meaningful parameter is the time (or RG flow parameter) t, thus our restriction to the diagonal g_{tt}. An arclength in the projective Hilbert space determined by a continuously parametrized unitary is defined (up to a universal constant) by $d_{FS}(\psi(t)) := \int_0^t dt' \sqrt{g_{tt}} = \int_0^t dt' \sigma_H(t')$. The efficiency of $U(t)$ with respect to flow state $\psi(t)$ is characterized by the ratio of the geodesic arclength to the arclength taken by U [45]:

$$\varepsilon(\psi(t)) := \frac{\cos^{-1}|\langle\psi(t)|\psi(0)\rangle|}{d_{FS}(\psi(t))} = \frac{\cos^{-1}|\langle\psi(t)|\psi(0)\rangle|}{\int_0^t dt' \sigma_H(t')}. \quad (13)$$

Put more plainly, the efficiency ε of a continuous unitary $U(t)$ with respect to an initial state $\psi(0)$ is the ratio of the geodesic distance between $(\psi(t), \psi(0))$, and the distance of the path from $(\psi(t), \psi(0))$ dictated by U.

Using Eq. (4) and the Fubini-Study definition of σ_H, we extract another upper bound on the entanglement entropy of the boundary state $\psi(t)$ via

$$E(\rho(t)) \leqslant 2\cos^{-1}(|\langle\psi(t)|\psi(0)\rangle|)\varepsilon(\psi(t))^{-1}\ln d_A. \quad (14)$$

That the entanglement entropy bound scales inversely with the efficiency is consistent with shallow-depth local quantum circuits obeying area-law entanglement.

Thus, we see that two components comprise our entanglement entropy bound in Eq. (4): A distance measure in the projective Hilbert space, and a complexity measure (IFC) particular to the bipartition. While the IFC is difficult to numerically obtain, the divergence between entanglement growth and unitary rotation becomes manifest, as we now explore in the context of MBL.

IV. WEGNER WILSON FLOW AND MBL

The entanglement analysis given above is applicable to any continuous unitary flow; however, our interests lie in one unitary particularly relevant to MBL and generating ℓ bits:

The Wegner Wilson flow. The WWF is fundamentally a diagonalization protocol that continuously evolves an orthonormal set of initial states into eigenstates of a given Hamiltonian. For Hamiltonian H_0 and initial basis $\{\psi_0\}$, the WWF is succinctly expressed by the differential equation

$$\frac{dU(\beta)}{d\beta} = \eta(\beta)U(\beta), \quad (15)$$

whereby we define $H(\beta) = U(\beta)H_0 U^\dagger(\beta)$ as the flow Hamiltonian. The term $\eta(\beta) = [H_d(\beta), H(\beta)]$ is the commutator of the diagonal component (with respect to the ψ_0 basis) of the flow Hamiltonian, $H_d(\beta)$, with $H(\beta)$. We define the variance of the WWF as $V(\beta) = \langle V_0(\beta)\rangle_0 := \langle(H(\beta) - H_d(\beta))^2\rangle_0$, where $\langle\cdot\rangle_0$ denotes averaging over $\{\psi_0\}$, and $V_0(\beta) = \langle\psi_0|(H(\beta) - H_d(\beta))^2|\psi_0\rangle$. The WWF ensures $V(\beta) \to 0$ monotonically; in particular, the decay of off-diagonal elements of $H(\beta)$ scales exponentially with $[\beta] =$ energy^{-2} [25,26]. Moreover, the WWF induces a geodesic flow with respect to the Fubini-Study metric given appropriate constraints on H_0 and $\{\psi_0\}$ [25], which motivated our discussion in Sec. III. Numerical studies have demonstrated the WWF produces more quasilocal integrals of motion in the MBL phase than other flow equation methodologies [18,46]. The WWF is also easier to implement, though it is susceptible to numerical stiffness issues [46].

As a testbed for our analytics, we consider the prototypical MBL Hamiltonian, the one-dimensional spin-1/2 Heisenberg model with on-site disorder and open boundary conditions.
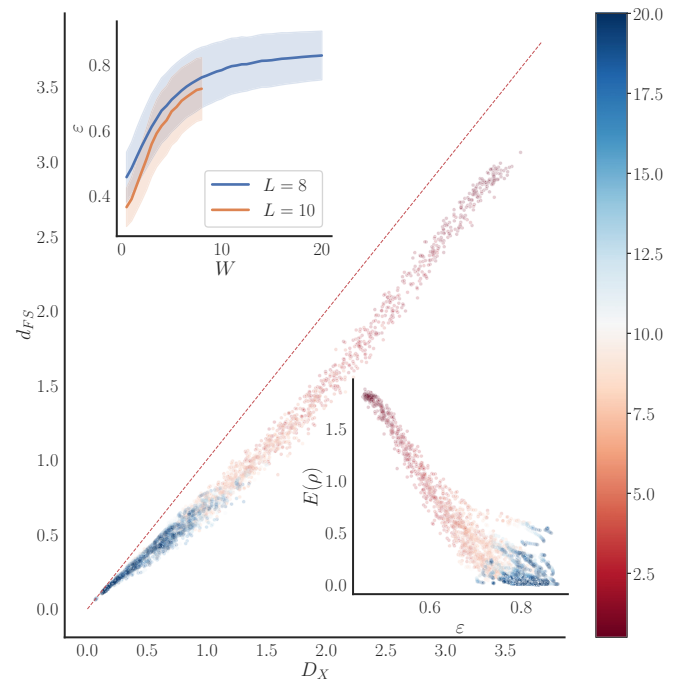

FIG. 2. Average WWF arclength d_{FS} against D_X for $L = 8$. Colors denote varying disorder strengths; the red diagonal line is a guide to the eye. (Left inset) Median efficiency against disorder strength W for both $L = 8$ and $L = 10$. Shading denotes standard deviation estimated via bootstrap sampling. (Right inset) Average entanglement entropy against WWF efficiency for $L = 8$, with color coding the same as the main plot.
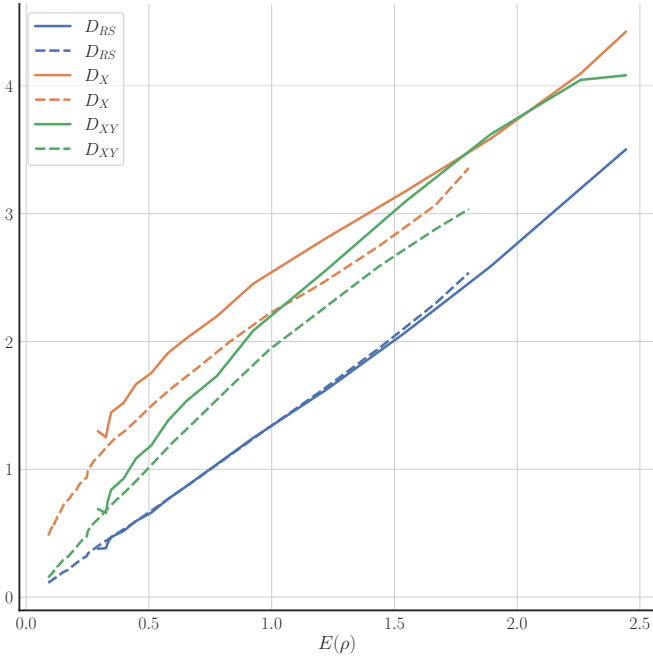
FIG. 3. The three bulk entanglement measures (D_{RS}, D_{XY}, D_X) against $E(\rho)$. The dashed lines denote $L = 8$, while the solid lines denote $L = 10$.

The Hamiltonian is given by

$$H = \frac{1}{4}\sum_i \boldsymbol{\sigma}_i \cdot \boldsymbol{\sigma}_{i+1} + \frac{h_i}{2}\sigma_i^z, \qquad (16)$$

where $h_i \in [-W, W]$ is sampled uniformly. A large body of numerical and theoretical work has placed the MBL transition in the thermodynamic limit at $W_c \approx 3.8$ for this model, though the dependence on system size has recently come into question [1,47,48]. We perform WWF in the zero magnetization sector and work within the computational σ_z basis. We utilize the same numerical procedure and tests for convergence outlined in previous works [18,22]. We performed our analysis on $L = 8$ and $L = 10$ system sizes, and average within a disorder realization before averaging over realizations. Due to calculating the IFC at each stage of the flow, we are relegated to smaller system sizes. For the case of $L = 10$, we choose to calculate the IFC at each flow step for only a subset of flow states. However, the qualitative results of our analytics given above is still clear.

Figure 2 depicts the median WWF efficiency [as defined in Eq. (13)] as a function of disorder, where we see a clear monotonic climb toward unity upon entering the MBL phase. This monotonicity is coincident with the increasing quasilocality of the integrals of motion: in the infinite disorder limit, the eigenstates are effectively product states, and therefore the flow is essentially geodesic with respect to the Fubini-Study metric. Figure 2 also shows d_{FS}, the average WWF arclength from initial to final state, against D_X, the root-mean WWF Fubini-Study arclength. By Jensen's inequality, D_X is larger than d_{FS}, though this inequality becomes parametrically weaker upon entering the MBL phase. Figure 2 further depicts the average entanglement entropy of the eigenstates against the
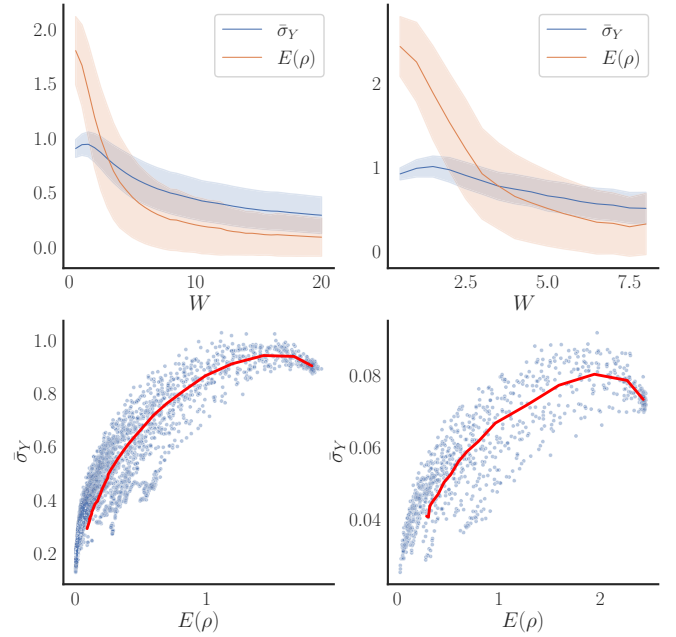

FIG. 4. (Top) Average (over flow states) IFC $\bar{\sigma}_Y$ and eigenstate entanglement entropy against disorder strength W for $L = 8$ (left) and $L = 10$ (right). Shading denotes standard deviation. (Bottom) Average IFC against $E(\rho)$ for $L = 8$ (left) and $L = 10$ (right). The points represent values averaged within a disorder realization, while the red line denotes the trend after averaging over disorder realizations.

WWF efficiency. Consistent with our claim above, a higher efficiency correlates with a lower entanglement entropy.

The Fubini-Study metric is intimately tied to the diagonalization rate of the WWF. In particular, we have

$$g_{\beta\beta}(\psi) = -\frac{1}{2}\frac{dV_0(\beta)}{d\beta}, \qquad (17)$$

where ψ is the flow state for initial state ψ_0 [22]. As the disorder terms $h_i\sigma_i^z$ are diagonal in the spin configuration basis, and $\lim_{\beta \to \infty} V_0(\beta) = 0$, the energy functional $\int g_{\beta\beta}d\beta \propto V_0(0)$ is independent of disorder strength or realization for every flow state ψ. Our recasting of the Fubini-Study metric then implies [22,26]

$$D_X = \int d\beta \left(-\frac{1}{2d}\frac{dV(\beta)}{d\beta}\right)^{1/2}. \qquad (18)$$

In Fig. 3, we depict D_X against the average eigenstate entanglement entropy $E(\rho)$ (we suppress the averaging notation for brevity), as well as $D_{RS} := \int \sigma_\eta\sigma_Y$, proportional to the integral of Eq. (4). We note that D_{RS} is strongly linear throughout the phase diagram, in strong contrast to D_X. The nonlinearity in D_X is most manifest for small $E(\rho)$ (large disorder strength W), as in the infinite disorder limit both $E(\rho)$ and D_X should approach zero.

The central difference between D_X and D_{RS} lies in σ_Y, the information fluctuation complexity (IFC). In Fig. 4, we depict the average IFC $\bar{\sigma}_Y$ (recall this average is over the flow trajectory, then over the set of eigenstates) against disorder strength W. We simultaneously plot $E(\rho)$ against W, and note that $E(\rho)$ decreases at a faster rate than $\bar{\sigma}_Y$. The lower panels

of Fig. 4, wherein we plot $\bar{\sigma}_Y$ against $E(\rho)$, more clearly shows the discrepancy. The consequence of this nonlinearity is that the degree of rotation quantified by D_X fails to linearly correlate with the degree of entanglement growth as the system enters the MBL phase. To phrase this differently, a measure of unitary rotation is inequivalent to a measure of entanglement growth.

This discrepancy is fundamentally tied to the distinction between $\eta(\beta)$ and $\eta_\partial(\beta)$, the terms in η that couples the degrees of freedom across the bipartition. Early in the flow, η_∂ is wellapproximated as a sum of local quadratic and quartic terms [23,26] and is therefore intensive, while η is extensive; thus, the entanglement bound D_X is poor for small β. As the flow progress, η couples degrees of freedom more and more distant from the bipartition cut, such that $||\eta_\partial||_\infty$ is wellapproximated by $||\eta||_\infty$. While η_∂ couples more nonlocal degrees of freedom late in the flow, the strength of those couplings exponentially decay with β, in correspondence to the decay of off-diagonal elements of H.

It is interesting to note that, in the context of cMERAs, the Fubini-Study/Bures metric serves as a suitable bulk measure for the entanglement entropy, unlike the nonlinear relation presented in Fig. 3. We suspect this difference stems from the cMERA hyperbolic geometry in the thermodynamical limit, in which geodesics (minimal surfaces) are lines extending into the bulk, and the Fubini-Study metric effectively measures the strength of disentanglers [29,30,35]. In the present WWF context, the unitary bulk represents an *energy diagonalization* flow, as reflected in the energy functional $V_0(0) = \int d\beta g_{\beta\beta}$;

the goal of the WWF is a projective Hilbert space trajectory such that $V(\beta)$ optimally decays. As demonstrated here, that goal is generally at odds with a flow that optimally generates entanglement. We leave open the question of whether a more natural bulk metrical construction quantifies the entanglement entropy generated by the WWF.

To briefly conclude, we investigated connections between the growth of entanglement entropy and quantum geometrical metrics. By giving a new proof to the small incremental entangling theorem, we established how bounds on entanglement entropy scale with the efficiency of the operators generating unitary evolution. Focusing on a prototypical MBL model, we numerically determined the degradation of boundary entanglement entropy bounds upon approximating key quantum informational functionals. We determined that the information fluctuation complexity is a pivotal quantity delineating unitary evolution from entanglement growth.

[1] A. Pal and D. A. Huse, Phys. Rev. B **82**, 174411 (2010).

[2] D. A. Abanin, E. Altman, I. Bloch, and M. Serbyn, Rev. Mod. Phys. **91**, 021001 (2019).

[3] V. Oganesyan and D. A. Huse, Phys. Rev. B **75**, 155111 (2007).

[4] M. Serbyn, Z. Papić, and D. A. Abanin, Phys. Rev. Lett. **111**, 127201 (2013).

[5] D. A. Huse, R. Nandkishore, and V. Oganesyan, Phys. Rev. B **90**, 174202 (2014).

[6] I. H. Kim, A. Chandran, and D. A. Abanin, arXiv:1412.3073.

[7] J. H. Bardarson, F. Pollmann, and J. E. Moore, Phys. Rev. Lett. **109**, 017202 (2012).

[8] J. Z. Imbrie, J. Stat. Phys. **163**, 998 (2016).

[9] W. De Roeck and J. Z. Imbrie, Philos. Trans. R. Soc. A **375**, 20160422 (2017).

[10] S. Roy and D. E. Logan, Phys. Rev. B **101**, 134202 (2020).

[11] D. Pekker and B. K. Clark, Phys. Rev. B **95**, 035116 (2017).

[12] X. Yu, D. J. Luitz, and B. K. Clark, Phys. Rev. B **94**, 184202 (2016).

[13] D. J. Luitz, Phys. Rev. B **93**, 134201 (2016).

[14] X. Yu, D. Pekker, and B. K. Clark, Phys. Rev. Lett. **118**, 017201 (2017).

[15] M. Žnidarič, T. Prosen, and P. Prelovšek, Phys. Rev. B **77**, 064426 (2008).

[16] M. Žnidarič, A. Scardicchio, and V. K. Varma, Phys. Rev. Lett. **117**, 040601 (2016).

[17] D. Pekker, B. K. Clark, V. Oganesyan, and G. Refael, Phys. Rev. Lett. **119**, 075701 (2017).

[18] V. K. Varma, A. Raj, S. Gopalakrishnan, V. Oganesyan, and D. Pekker, Phys. Rev. B **100**, 115136 (2019).

[19] V. L. Quito, P. Titum, D. Pekker, and G. Refael, Phys. Rev. B **94**, 104202 (2016).

[20] A. Chandran, J. Carrasquilla, I. H. Kim, D. A. Abanin, and G. Vidal, Phys. Rev. B **92**, 024201 (2015).

[21] T. B. Wahl, A. Pal, and S. H. Simon, Phys. Rev. X **7**, 021018 (2017).

[22] X. Yu, D. Pekker, and B. K. Clark, arXiv:1909.11097.

[23] S. J. Thomson and M. Schiro, SciPost Physics, **11** 39 (2021).

[24] C. J. Cao, S. M. Carroll, and S. Michalakis, Phys. Rev. D **95**, 024031 (2017).

[25] Y. Itto and S. Abe, Found. Phys. **42**, 377 (2012).

[26] C. Monthus, J. Phys. A: Math. Theor. **49**, 305002 (2016).

[27] F. Pastawski, B. Yoshida, D. Harlow, and J. Preskill, J. High Energy Phys. 06 (2015) 149.

[28] M. Miyaji and T. Takayanagi, Prog. Theor. Exp. Phys. **2015**, 073B03 (2015).

[29] X.-L. Qi, arXiv:1309.6282.

[30] B. Swingle, Phys. Rev. D **86**, 065007 (2012).

[31] E. Witten, Adv. Theor. Math. Phys. **2**, 253 (1998).

[32] J. Maldacena, Int. J. Theor. Phys. **38**, 1113 (1999).

[33] K. Hyatt, J. R. Garrison, and B. Bauer, Phys. Rev. Lett. **119**, 140502 (2017).

[34] T. Zhou and A. Nahum, Phys. Rev. B **99**, 174205 (2019).

[35] M. Nozaki, S. Ryu, and T. Takayanagi, J. High Energy Phys. 10 (2012) 193.

[36] K. Van Acoleyen, M. Mariën, and F. Verstraete, Phys. Rev. Lett. **111**, 170501 (2013).

[37] S. Bravyi, Phys. Rev. A **76**, 052319 (2007).

[38] A. Vershynina, J. Math. Phys. **60**, 022201 (2019).

[39] A. Hutter and S. Wehner, Phys. Rev. Lett. **108**, 070501 (2012).

[40] J. Bates and H. Shepard, Phys. Lett. A **172**, 416 (1993).

[41] H. Jürgensen and D. E. Matthews, Journal of Universal Computer Science **16**, 749 (2010).

[42] M. R. Dowling and M. A. Nielsen, arXiv:quant-ph/0701004.

[43] S. Chapman, M. P. Heller, H. Marrochio, and F. Pastawski, Phys. Rev. Lett. **120**, 121602 (2018).

[44] T. Neupert, C. Chamon, and C. Mudry, Phys. Rev. B **87**, 245103 (2013).

[45] C. Cafaro, S. Ray, and P. M. Alsing, Phys. Rev. A **102**, 052607 (2020).

[46] S. Savitz and G. Refael, Phys. Rev. B **96**, 115129 (2017).

[47] D. J. Luitz, N. Laflorencie, and F. Alet, Phys. Rev. B **91**, 081103(R) (2015).

[48] J. Šuntajs, J. Bonča, T. c. v. Prosen, and L. Vidmar, Phys. Rev. E **102**, 062144 (2020).